Onset of chaos in a pendulum coupled to a thermal environment

S. Fahy, S. Twohig, M. Stefansson, and D. Courtney
Department of Physics, University College, Cork, Ireland
(Received 16 October 1997)

We consider the onset of chaos in a pendulum driven by a Brownian noise environment. The behavior of the Lyapunov exponents of the system as a function of the strength of the coupling to the thermal environment is investigated for two models of thermal coupling (given by the Langevin equation and by random stop-start motion). For sufficiently strong coupling to the environment, the motion is nonchaotic and almost all trajectories are stable but, for each initial velocity and realization of the Brownian noise, an exceptional set of unstable trajectories exists, in analogy to the existence of basin boundaries in deterministically driven systems. The initial points of the unstable trajectories form a fractal set, the dimension of which is zero for coupling to the environment greater than a (temperature-independent) critical value, grows as the environmental coupling is decreased, and equals one at the transition to chaotic behavior. [S1063-651X(98)08403-7]

PACS number(s): 05.45.+b, 05.40.+j, 02.50.Ey

I. INTRODUCTION

In this paper, we analyze the dynamical behavior of a simple pendulum, the motion of which is driven by Brownian forces only. In particular, we will be concerned with the onset of chaos in such a system. The study of chaotic behavior in a variety of randomly driven systems has recently attracted some interest, motivated both by the aim of a deeper understanding of Brownian motion and also by an interest in the synchronization effects of a common source of external noise on a pair of (coupled or uncoupled) dynamical systems [1–13]. The study of such problems lies between the traditional domains of statistical mechanics and nonlinear dynamics. The simple pendulum is one of the most important prototypes of nonlinear motion in classical mechanics and is a natural candidate for study as a randomly driven system.

The presence or absence of chaos in randomly driven systems may be phrased in terms of the question: given two uncoupled dynamical systems subjected to a common external random driving force (a common ''thermal environment''), to what extent are their final states similar? Equivalently, one may ask the question: for a specific history of the thermal environment (i.e., a specific realization of the random external forces), is the final condition of the system at large times sensitive to its initial condition or is it determined solely by the history of the environment? A system sensitive to its initial condition is said to be chaotic; a system determined solely by its environment is nonchaotic.

Both in the general case of dynamical systems with randomly varying parameters [3,6] and, in the specific case of Brownian motion [4], these questions have been addressed previously in terms of the expected Lyapunov exponent along a typical trajectory of the system and in terms of intermittent bursting of snapshot attractors [3] in the chaotic regime. It has been shown [4,8] that, in the limit of very strong coupling to the environment, the motion of the system at large times is determined entirely by the noise and is independent of the initial state of the system. For sufficiently weak coupling to the environment, the state of motion of the system at large times is sensitive to its initial condition and is not determined solely by the realization of environmental noise. However, to our knowledge, it has not been directly explored how the dynamics of a randomly driven system evolves towards chaos within the nonchaotic regime, as a system control parameter (e.g., the coupling to the environment) is varied. Specifically, to what extent can one identify precursors of chaotic behavior *in the nonchaotic regime* for a randomly driven system?

From the point of view of conventional nonlinear dynamics, one is faced with a number of difficulties in studying a randomly driven system: (1) The perturbation due to the thermal environment is not a ''small'' addition to a regular, deterministic driving force—in fact, the thermal noise is the *only* stimulus of motion and, without it, the system remains static at a point of stable equilibrium. Thus, analysis of the dynamics of the unperturbed, deterministic system gives limited insight into the behavior of the noisy system. (2) in contrast to well-defined phase-space structures such as attractors, basins of attraction, and separatrices, which serve to classify the asymptotic trajectories of deterministic systems, the phase-space dynamics of a thermally driven system are apparently quite featureless; the motion is usually ergodic and the asymptotic occupation of the phase space can be characterized entirely by the Boltzmann distribution for the appropriate temperature. (3) Because noise is dominant in the dynamics, analysis in terms of return maps yields featureless and uninformative results. (4) In the understanding of routes to chaos, phenomena such as period doubling or intermittency cannot be expected since the driver of the system (i.e., the thermal environment to which the system is coupled) has a complex, random behavior, which is specified only in statistical terms and in which no periodic behavior is evident.

A satisfactory approach to the analysis of chaos in randomly driven systems, which partially overcomes some of the difficulty in addressing items (1) and (2) of the previous paragraph, involves the use of what we may call ''specific realizations'' of the thermal environment [1,3,4]. In practice, by this we mean that a *specific* sequence of random forces (or impulses) is chosen from the appropriate distribution for the thermal environment, specifying the exact values of the thermal forces over a sufficiently long-time interval. Once this is done, we now have a deterministic problem, albeit one with a highly complex sequence of driving impulses. The

behavior of the system subjected to this specific realization of the thermal environment is then analysed (e.g., the time-averaged Lyapunov exponents may be calculated or separatrices may be identified, as discussed below). In order to obtain statistically relevant properties, this entire analysis (i.e., choice of specific sequence of random forces over a long-time interval, followed by analysis of the resulting driven system) must be repeated many times and the appropriate average over the driven systems obtained. (For some properties, e.g., the Lyapunov exponents, time averaging is equivalent to ensemble averaging and a single long-time realization of the thermal forces is sufficient to give the appropriate averages.) This approach may thought of as applying a ''common noise'' signal to an ensemble of systems, each member of the ensemble having a different set of initial conditions. Indeed, an important physical application of the analysis of chaos in randomly driven systems is to the understanding of synchronization of uncoupled systems effected by common noise signals.

The behavior of the simple pendulum subjected to a sinusoidal driving force has been well studied [12] and displays rich, well-defined phase-space structures, e.g., basins of attraction, with their associated attractors and separatrices. A system driven by Brownian forces can be classified [4,8,10] as chaotic or nonchaotic, depending on whether its largest (average) Lyapunov exponent is positive or negative, respectively, in a very similar way to the deterministically driven systems. However, it is of interest to know whether any analogs of the phase-space structures present for the simpler, sinusoidally driven pendulum are also present for the pendulum driven by Brownian forces, and whether such structures evolve in a systematic way as the control parameters (e.g., the strength of coupling to the environment) are changed. In this paper, we concentrate principally on the behavior of the pendulum driven by Brownian forces in the nonchaotic regime. Despite the difficulties in analyzing phase-space structures for randomly driven systems that we cited above, we will demonstrate the existence of structures that are analogous to the boundaries (or separatrices) between basins of attraction in the sinusoidally driven pendulum, and quantify the changes in those structures as the coupling to the environment decreases and the system evolves towards chaos.

The remaining sections of this paper are organized as follows: In Sec. II, we consider the motion of a particle of mass m, confined to move in one dimension, coupled to a thermal environment consisting of a gas of particles of mass m'. This provides a physical model of one-dimensional Brownian motion [10]. Two limiting cases of this physical model will subsequently be used in the analysis of Brownian motion of the simple pendulum. Numerical results obtained from simulations of Brownian motion of the pendulum are presented in Sec. III and some relevant analytic results are proven in Sec. IV. The overall conclusions of this study are discussed in Sec. V.

II. PHYSICAL MODEL OF THERMAL MOTION

In this section we consider a simple, microscopic mechanical model of Brownian motion in one dimension. The properties of this model have been investigated in detail in Ref. [10] and we give only a survey of relevant properties here. Brownian motion is usually modeled using the Langevin equation [13,14], in which the particle is considered to be moving in a viscous medium, with a viscous force proportional to velocity, while subjected to random impulses from the microscopic thermal motion of the medium. Although this is the standard mathematical representation of Brownian motion, it is not an explicit, fully microscopic mechanical model of the physical motion since, at the microscopic level, all collisions with the particles of the medium are elastic and viscous damping merely represents the time-averaged transfer of momentum from the particle under consideration to other particles in the system.

As we will see in this section, the Langevin equation is by no means the only valid mathematical representation of the physical process of Brownian motion. The physical model we introduce below includes the Langevin equation as a special limiting case. It also includes the other mathematical model of thermal coupling (so-called stop-start motion [4,15]), which we will find convenient to use in our subsequent analysis of chaotic behavior in the pendulum coupled to a thermal environment. Indeed, there is a wide range of physically valid mathematical models of Brownian motion. It is important, therefore, that the qualitative physical results one obtains in the mathematical analysis of the motion should not depend on the specific mathematical model of Brownian motion chosen.

The physical model of thermal coupling [10] is as follows: We consider a particle of mass m moving in one dimension, colliding intermittently with the particles of a surrounding gas, each of mass m'. We assume that the distribution of velocities of the particles m' is Maxwellian, so that their mean velocity $\langle v' \rangle = 0$ and $m' \langle (v')^2 \rangle = k_B T$, where T is the absolute temperature of the system, k_B is the Boltzmann constant, and $\langle X \rangle$ represents the thermal average of a quantity X. Consider a single elastic collision between the particle of mass m, with velocity v_1 before the collision, and one of the other particles m', with velocity v_1'. An elementary calculation, using conservation of energy and momentum, shows that the velocity v_2 of the particle of mass m after the collision is given by

$$v_2 = \frac{m-m'}{m+m'} v_1 + \frac{2m'}{m+m'} v_1' . \tag{1}$$

After n collisions (in the absence of other forces on the particle m), its velocity v_{n+1} is given by

$$v_{n+1} = \left[\frac{m-m'}{m+m'}\right]^n v_1 + \frac{2m'}{m+m'} \sum_{j=1}^{n} \left[\frac{m-m'}{m+m'}\right]^{n-j} v_j' ,$$

where v_j' is the velocity of the particle of mass m' in the jth collision.

Assuming the v_j' are independent and identically distributed (with mean zero and variance $k_B T/m'$) it then follows from the central limit theorem that, as $n \to \infty$, v_n has a Gaussian distribution with $m \langle (v_n)^2 \rangle = k_B T$. This is as one would expect on general thermodynamic grounds, since the particle of mass m is a classical system in thermal contact (via the collision process) with a reservoir (the collection of particles of mass m') at temperature T. Indeed, this general thermodynamic argument shows that, if the particle of mass

m experiences an additional force $-\partial V/\partial x$ due to an external potential $V(x)$, where x is the position of the particle m, the probability distribution of x at large times is given by the Boltzmann distribution $\exp[-V(x)/k_BT]/Z$, where the partition function $Z=\int \exp[-V(x)/k_BT]dx$. Thus, the asymptotic distribution of position and velocity of the particle m depends only on T and does not depend on the strength of its coupling to its surrounding environment. This coupling strength is determined by the mass m' of the particles in the environment and the average rate at which the particle m collides with them. Nevertheless, as we shall see in Secs. III and IV below, the strength of the coupling of the particle m to its thermal environment does affect the sensitivity of the particle's actual final trajectory to its initial position, given a specific realization of the thermal environment (i.e., a specific sequence of velocities $\{v_i'\}$).

In order to obtain the standard Langevin equation from the equations of motion defined by Eq. (1), we assume that the mass m' is much less than m and that the time Δt between collisions is small. The viscous drag is then proportional to the ratio $m'/\Delta t$. From Eq. (1) we see that the change in velocity of m in a single collision is given by

$$\Delta v = \frac{2m'}{m+m'}\,(v'-v),$$

where v is the its initial velocity and v' is the velocity of the particle with which it collides. Taking the limit, $m'\to 0$ and $\Delta t\to 0$, keeping

$$\frac{m'}{\Delta t}=\frac{m\gamma}{2}, \tag{2}$$

where γ is a constant, we obtain the Langevin equation [14],

$$\frac{dv}{dt}=-\gamma v+\eta(t), \tag{3}$$

where $\eta(t)$ is Brownian white noise with $\langle \eta(t)\eta(t')\rangle = 2\gamma k_BT\delta(t-t')/m$. If the particle m experiences an additional conservative force from an external potential $V(x)$, Eq. (3) becomes

$$\frac{d^2x}{dt^2}=-\frac{1}{m}\frac{\partial V}{\partial x}-\gamma\frac{dx}{dt}+\eta(t). \tag{4}$$

Another useful and natural limit of Eq. (1) occurs when $m'=m$, i.e., when the particles of the surrounding medium have the same mass as the particle m. In this case the particles m and m' exchange velocities in each collision. Considering only the motion of m, we then obtain the so-called stop-start Brownian motion [4,15], where the velocity of m is reset at the nth collision and replaced with a velocity v_{n+1}, chosen at random from a Maxwell distribution at temperature T. In the simulation of this type of motion, below, we make the further assumption that the collisions occur at regular intervals of $\Delta t=\tau$. In this motion, no damping is explicitly introduced and the particle m moves conservatively in the potential $V(x)$ in the intervals between collisions. This form of motion has been used in the Monte Carlo sampling of auxiliary fields in lattice gauge theories [15] and other interacting lattice fermion problems [16].

In the analysis of the chaotic behavior of the pendulum coupled to a thermal environment, stop-start motion proves to be somewhat more formally simple than Langevin motion. In stop-start motion, the phase space of the pendulum motion can be taken to be one dimensional, as follows: The initial velocity v_n for the nth step (i.e., the time interval between the $n-1$ collision and the nth collision) is chosen at random from a Maxwell velocity distribution for temperature T. The nth step is then a mapping $x(t=n\tau-\tau)\to x(t=n\tau)$ produced by integrating Newton's equations of motion for the (undamped) pendulum motion with initial velocity $dx/dt=v_n$. Thus, the phase space for the motion is one dimensional because the state of the system (i.e., the pendulum) is specified by $x(n\tau)$ alone and the velocities v_n play the role of parameters of the environmental driver, rather than phase-space coordinates of the driven system. We may then view the evolution of the system from $t=0$ to $t=n\tau$ as a product of n randomly chosen mappings of the circle onto itself.

On the other hand, the phase space of the Langevin motion of the pendulum is two dimensional, with phase space coordinates $x(t)$ and $v(t)=dx/dt$, as is the case for the usual damped simple pendulum [12]. The evolution of the system from its initial state $[x(t=0),\ v(t=0)]$ to its final state $[x(t),\ v(t)]$ is specified by Eq. (4), once a particular (random) choice of the forcing term $\eta(t')$ for $0\leqslant t'\leqslant t$ has been made. Although the damped system is two dimensional, we will find it convenient to consider the evolution of the constant velocity slices of initial conditions, specified by $dx/dt=$ constant at $t=0$. All such slices are equivalent (assuming ergodicity of the motion) for the topological considerations below and this approach emphasizes the essential similarity to stop-start motion. Thus, when we refer to a particular ''noise realization'' for the damped motion, we assume that the initial velocity slice has been specified (with velocity chosen from a Maxwell distribution) along with the realization of the forcing term, $\eta(t')$ for $0\leqslant t'\leqslant t$.

Although Langevin motion and stop-start motion appear quite different in their detailed implementation of the thermal coupling, many of the results that are obtained from each are remarkably similar, if the stop-start coupling with interval τ between collisions is compared with the Langevin coupling with viscous coefficient $\gamma=2/\tau$. This relation between τ and γ is obtained from Eq. (2), by setting $m=m'$ and $\tau=\Delta t$. We will discuss this relation further in Sec. IV, below. The fact that the coupling to the environment is intermittent and abrupt in the stop-start motion while it is continuous in the Langevin motion has a relatively minor effect on the results, particularly at higher temperatures. The numerical results in Sec. III and the analytical results in Sec. IV are strikingly similar in every regard for both forms of motion. For this reason, it would seem that the qualitative nature of the results below have much wider applicability than to the two models explicitly analyzed and it is likely that any physically sensible coupling of the pendulum to a thermal reservoir would reveal qualitatively similar behavior.

III. NUMERICAL RESULTS

We have performed numerical simulations of both the Langevin and the stop-start models of Brownian motion of

the simple pendulum. In the presentation that follows, we set the mass $m=1$ and use the variable $x=\theta/2\pi$, where θ is the angle of the pendulum to the downward vertical. The potential $V(x)=-\cos[2\pi x]/2\pi$, so that V has a period of 1 in the variable x.

For stop-start motion, the equation of motion during each step (i.e., between consecutive collisions) is that for free motion of the pendulum: $d^2x/dt^2=-\sin[2\pi x]$. Numerical integration was performed by the standard ''leap-frog'' method [15]. A leap-frog integration time step of approximately 0.02 was found to give well-converged results for the integration of the equations of motion. The sequence of initial Gaussian velocities v_n (with variance k_BT) for each step was generated by a Box-Muller transformation of uniform pseudorandom numbers generated by a double (64-bit) precision floating point version of the subroutine ''RAN3'' given in Ref. [17], which is based on the subtractive pseudorandom number generator of Knuth [18]. The coordinate x was represented in machine quadruple (128-bit) precision for the analysis of the fractal structure of ''breaks'' (see below) although, for the calculation of other quantities, double precision is sufficient. In stop-start motion, the specific realization of the environment is determined by the sequence of random velocities $\{v_n\}$, which is determined by the initial seed of the pseudorandom number generator.

For the damped motion, the Langevin equation, Eq. (4), is numerically integrated using the following modification of the leap-frog method, which explicitly includes damping. Let s be the integration time step. Given the position $x(t)$ and velocity $v(t)$ at time t, the position $x(t+s)$ and velocity $v(t+s)$ at time $t+s$ are generated as follows: A random impulse, $\delta v=\sqrt{2\gamma s k_BT}\zeta$, where ζ is a Gaussian random variable with unit variance, is applied to the velocity at time t: i.e., $v(t^+)=v(t^-)+\delta v$. The velocity at the time $t+(s/2)$ is then found by analytically integrating

$$\frac{dv}{dt'}=F-\gamma v(t') \tag{5}$$

over the interval $t<t'<t+(s/2)$, taking $F=-\partial V/\partial x$ at $x=x(t)$ to be constant over this interval. This gives

$$v(t+s/2)=\exp[-\gamma s/2]v(t^+)-\frac{1-\exp[-\gamma s/2]}{\gamma}\left.\frac{\partial V}{\partial x}\right|_{x=x(t)}.$$

The position at time $t+s$ is then

$$x(t+s)=x(t)+sv(t+s/2), \tag{6}$$

and the velocity at time $t+s^-$ (just before the next velocity impulse) is found by integrating Eq. (5) over the interval $t+s/2<t'<t+s$, taking $F=-\partial V/\partial x$, at $x=x(t+s)$ from Eq. (6), to be constant over this interval, so that

$$v(t+s^-)=\exp[-\gamma s/2]v(t+s/2)-\frac{1-\exp[-\gamma s/2]}{\gamma}\left.\frac{\partial v}{\partial x}\right|_{x=x(t+s)}.$$

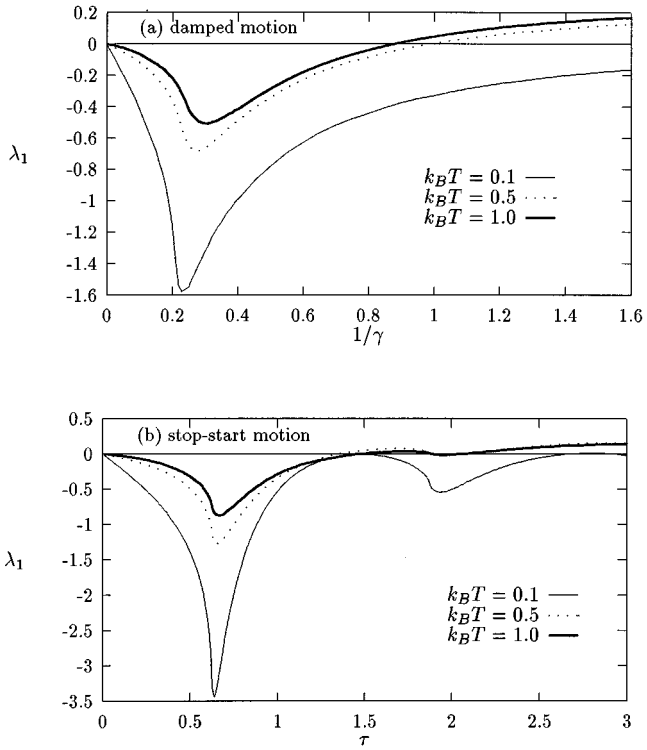

FIG. 1. The Lyapunov exponent λ_1 of the thermally driven pendulum as a function of inverse environmental coupling strength, (a) $1/\gamma$ for damped motion, and (b) τ for stop-start motion, at temperatures $k_BT=0.1$, 0.5, and 1. In (a) λ_1 is the larger Lyapunov exponent; in (b) there is only one exponent.

This completes the integration of the damped equations of motion over the integration time step $[t,t+s]$. In the limit, $\gamma\to 0$, this procedure reduces to the usual leap-frog integration method.

In the Langevin implementation of the thermal coupling, the specific realization of the environment is determined by the sequence of velocity impulses $\{\delta v\}$ applied at times $t=s,2s,3s,\ldots$ which, as in the case of stop-start motion, is determined by the initial seed of the pseudorandom number generator. As mentioned in Sec. II, the initial velocity slice $v(t=0)$ for Langevin motion was chosen from a Maxwell distribution. For each value of the damping coefficient γ the integration time step s used was $0.1/\gamma$. (Some integrations were carried out with a time step s of $0.05/\gamma$, with negligible change in results.)

A. Average Lyapunov exponents

Shown in Fig. 1 is the Lyapunov exponent versus inverse environmental coupling, numerically calculated for both types of motion at various environment temperatures. For the damped motion, the larger Lyapunov exponent [19] (shown) was calculated from the ensemble average,

$$\lambda_1=\frac{1}{t-t_0}\int_0^1 dx\int_{-\infty}^{+\infty}dv\left\langle \ln\left\{\frac{|\Delta x(t)|}{|\Delta x(t_0)|}\right\}\right\rangle_{\delta v} P[x,v], \tag{7}$$

by integrating the equation of motion, Eq. (4), for initial values,

$$[x_1(t=0),v_1(t=0)]=[x-\xi/2,v] \quad \text{and}$$

$$[x_2(t=0),v_2(t=0)]=[x+\xi/2,v],$$

where $\xi=10^{-4}$. On each integration time step, the impulse δv given to v_1 was the same as that given to v_2. The difference $\Delta x(t')$ is equal to $[x_2(t')-x_1(t'),v_2(t')-v_1(t')]$. For each value of (x,v), $\langle \ln\{|\Delta x(t)|/|\Delta x(t_0)|\}\rangle_{\delta v}$ denotes the average value of $\ln\{|\Delta x(t)|/|\Delta x(t_0)|\}$ from 4 statistically independent realizations of the noise sequence $\{\delta v\}$ over the time interval $[0,t]$. Each integration was carried out for a total time of $t=100/\gamma$ and $t_0=4/\gamma$. If the distance $|\Delta x(t')|$ became greater than 10^{-4} or less than 10^{-10} at any time t', it was rescaled to equal 10^{-7} and the rescaling factor accounted for in the calculation of λ_1. The asymptotic distribution $P[x,v]$ of the positions and velocities is given by the Boltzmann distribution,

$$P[x,v]=\frac{\exp[-(V(x)+v^2/2)/k_BT]}{\sqrt{2\pi k_BT}\int_0^1 \exp[-V(x)/k_BT]dx}.$$

For the stop-start motion, the phase space of the system is one dimensional and the Lyapunov exponent shown in Fig. 1 was found by evaluation of the ensemble average,

$$\lambda=\frac{1}{\tau}\int_0^1 dx(0)\int_{-\infty}^{+\infty} dv\ \ln\left[\left|\frac{\partial x(\tau)}{\partial x(0)}\right|_{x(0)=v}\right]P[x(0),v], \tag{8}$$

of the length expansion factor $\ln[|\partial x(\tau)/\partial x(0)|_{v(0)=v}]$ for a single time interval τ between collisions. In this expression, $x(0)$ is the position at the start and $x(\tau)$ is the resulting position at the end of the time interval τ, given that the initial velocity $v(0)=v$. The derivative $|\partial x(\tau)/\partial x(0)|_{v(0)=v}$ was found by integrating the (undamped) motion over one time interval τ for initial values, $x_1(t=0)$ and $x_2(t=0)$, a distance 10^{-7} apart.

A fixed grid in x and v (rather than a Monte Carlo sampling [4]) is used for the numerical evaluation of the integral in Eqs. (7) and (8). The grid spacing in x is uniform on the interval [0,1] and a nonuniform grid of v is used, where the spacing Δv between consecutive grid values of v is chosen so that $\Delta v\ \exp[-v^2/2k_BT]$ is constant. A grid of 100×100 points was found to give very well converged values for the integrals. Particularly for large values of γ or small values of τ, this ensemble-average method of evaluating λ is more numerically efficient than the time-average method, where one calculates the average scaling rate over a single, very long trajectory. We have checked, for a number of values of γ, τ, and T, that the values of λ obtained from ensemble averaging are the same as those from time averaging.

The principal features of λ as a function of inverse environmental coupling strength (τ or $1/\gamma$) are the presence of a deep minimum near $\tau=0.6$ or $1/\gamma=0.25$ and a crossing to positive values near $\tau=1.5$ or (for higher temperatures) $1/\gamma=0.9$. The minimum is deeper for stop-start motion, particularly at low temperatures, for which the curve exhibits a second local minimum near $\tau=1.8$. For higher temperatures, the transition to chaotic behavior occurs at larger values of the coupling to the environment (i.e., smaller inverse coupling strength) for both forms of motion.

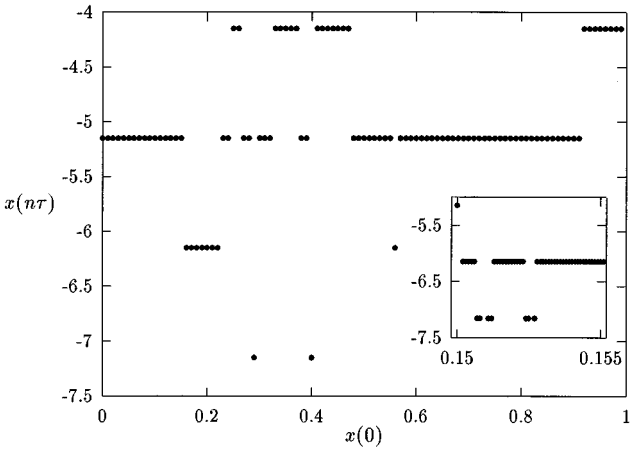

FIG. 2. Final coordinate $x(n\tau)$ vs initial coordinate $x(0)$ for stop-start motion with $\tau=1$, using a particular selection of random velocities $\{v_1,v_2,\ldots,v_n\}$. The total integration time was $n=500$ and the temperature was $k_BT=1$. The points on the main graph are for 100 equally spaced values of $x(0)$. The inset shows the graph for grid spacing $\epsilon=10^{-4}$ near the first break in the main figure.

B. Exceptional trajectories

The above calculations, giving a negative average Lyapunov exponent of the system for strong coupling to the environment, predict the long-time stability of *typical* trajectories, given a particular realization of the thermal environment. If the largest average Lyapunov exponent of the system is negative (as is the case for large γ or small τ), then typical Brownian trajectories are stable and, hence, are insensitive to small changes in initial conditions. Even for large changes in initial conditions, given a particular realization of the thermal impulses (i.e., the sequence $\{v_n\}$ for stop-start motion or the sequence $\{\delta v\}$ for Langevin motion), the final physical trajectory at large times is found to be independent of the initial conditions of the pendulum. However, although this is the case for *almost* all trajectories (in the statistical sense), it is not true for all. For each realization of the thermal impulses, there is at least one initial condition (and, in general, infinitely many) which gives rise to an unstable trajectory, for which the derivative $dx(t)/dx(0)\to\infty$ as $t\to\infty$. These unstable initial conditions have zero statistical weight and do not contribute to the average Lyapunov exponent λ, but their presence is an important precursor of the onset of chaos as $\lambda\to0$, as we shall see in the following analysis.

Shown in Fig. 2 is the graph of the final coordinate $x(n\tau)$ versus initial coordinate $x(0)$ for large n, obtained with stop-start motion using a specific, representative selection of Maxwell distributed velocities $v_1,v_2,\ldots,v_n$. [Qualitatively similar results are obtained in damped motion for $x(t)$ versus $x(0)$ for constant initial velocity slices.] Almost all points on the graph have values of $x(n\tau)$, which differ only by an integer, and correspond to the same final physical state of the pendulum. The step length τ was chosen such that the expected Lyapunov exponent is negative and $dx(n\tau)/dx(0)\to0$ as $n\to\infty$ for almost all $x(0)$; thus, the graph (see Fig. 2) is flat almost everywhere. However, by including the full value of x (not just its physically relevant fractional part) we see that the graph in Fig. 2 contains a set of ''breaks'' (points

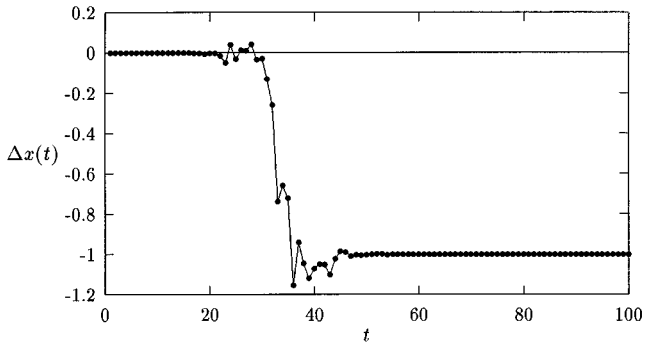

FIG. 3. Separation $\Delta x(t)=x_2(t)-x_1(t)$ vs time t for two points on opposite sides of a discontinuity (''break'') in the graph shown in Fig. 2. The initial separation $\Delta x(0)=10^{-6}$.

at which the graph is discontinuous) which are the boundaries between the basins of attraction for final values of x which differ by a nonzero integer.

The existence of at least one such break (both for stop-start motion and for any constant initial velocity slice in damped motion) is ensured by the periodic character of the potential $V(x)$: since trajectories starting at $x_1(0)=0$ and at $x_2(0)=1$ experience identical forces throughout their motion, their trajectories always remain precisely one period apart; i.e., $x_2(t)-x_1(t)=1$ for all t. This is immediately clear from the fact that the two trajectories in x correspond to identical trajectories of the physical system. The equivalent statement in terms of the physical variable θ for pendulum motion, which has the topology of a circle, is that the non-simply-connected topology of the circle $\theta(t=0)$ does not allow it to be mapped onto a single point $\theta(t\rightarrow\infty)$ without at least one break (point of discontinuity) occurring. In terms of the physical variable θ, there is only one basin of attraction, so that the breaks are not basin boundaries for the physical system in the usual sense. However, the physical trajectories of the pendulum, by which different initial points reach the final state, change winding number abruptly at the discontinuities in $x(t\rightarrow\infty)$ and the breaks define initial points of exceptional trajectories along which the Lyapunov exponent of the randomly driven system is positive.

We emphasize that the mapping given by each step, $x(n\tau-\tau)\rightarrow x(n\tau)$, is continuous and that it is only in the limit $n\rightarrow\infty$ that the graph is strictly discontinuous. However, the numerical simulations show that ''breaks'' typically emerge (i.e., are resolved at any given level of numerical accuracy) over a short interval in the evolution of the system and remain intact for all later times. To see this, we examine the separation $\Delta x(t)=x_2(t)-x_1(t)$ versus time t (see Fig. 3) for two close initial conditions, $x_1(0)$ and $x_2(0)$, on opposite sides of a discontinuity (''break'') in the graph of $x(t\rightarrow\infty)$ versus $x(t=0)$. At small times $\Delta x(t)$ is approximately zero. Over a short interval of time (e.g., from $t\approx 20$ to $t\approx 45$ in Fig. 3), we find that $\Delta x(t)$ changes abruptly to a nonzero value, close to its final value $\Delta x(t\rightarrow\infty)=m$, which is an integer.

The formation of the break illustrated in Fig. 3 is typical of the break formation found for the models considered here. During a typical interval, $x_1(t)$ and $x_2(t)$, adjacent points at $t=0$ on a uniform grid with spacing ϵ, converge exponentially since the *average* Lyapunov exponent along a typical trajectory is negative. However, fluctuations in the Lyapunov exponent occur and it may remain positive for some substantial interval. Over this confined interval of time $x_1(t)$ and $x_2(t)$ may diverge sufficiently from each other [20] that their separation becomes comparable to 1. (This occurs when the trajectory happens by chance to spend a long time near an unstable equilibrium $x=n+1/2$.) After that time $x_1(t)\pm 1$ may come close to $x_2(t)$ and remain so for all times after, no subsequent fluctuation in the Lyapunov exponent being sufficiently large to overcome the average negative value that causes $x_1(t)\pm 1$ to converge exponentially to $x_2(t)$. At the level of resolution defined by the grid spacing, ϵ, we may then say that a break occurs between $x_1(0)$ and $x_2(0)$.

If we now wish to locate the position of the break at a higher level of resolution and consider the evolution of a finer uniform grid of m points (with spacing ϵ/m) initially lying between $x_1(0)$ and $x_2(0)$, it immediately becomes clear that the structure of breaks has a statistically self-similar structure, as follows: Once $x_1(t)\pm 1$ has converged close to $x_2(t)$ (at some time $t_0>0$), the m points that initially lay between $x_1(0)$ and $x_2(0)$ have been stretched around the entire circle. (We note again that this stretching in practice occurs over a relatively confined interval in the evolution of the system—see Fig. 3.) The dynamics of the system (determined by the selection of velocities v_n) is statistically homogeneous in time, since all v_n are identically distributed random variables. Thus, the evolution of the finer grid on $[x_1(0),x_2(0)]$ (which has been stretched to the full circle at $t=t_0$) and the structure of breaks formed on that interval after $t=t_0$ is essentially identical to that of the coarser grid on $[0,1]$ after $t=0$.

Thus, what appears as a single break on an ϵ grid may appear composed of many ''sub-breaks'' on a finer (ϵ/m) grid (see Fig. 2). Although the specific number of breaks and the positions at which they appear in the grid depends on the specific realization of the thermal environment (i.e., the series of velocities $\{v_1,v_2,\ldots\}$ chosen), the structure of breaks must appear statistically similar at all levels of resolution. Because of the way in which breaks are formed by the random dynamics, the formation of breaks on finer grids corresponds to dynamics at later stages of evolution of the system. This is analogous to the formation of fractal basin boundaries for the sinusoidally driven pendulum [12,21].

In the Langevin implementation of thermal coupling, the breaks we identify are the intersection of the constant initial velocity slice $v(0)=v$ with the fractal basin boundaries of the system driven by the sequence of impulses $\{\delta v\}$. Each basin corresponds to initial conditions that lead to final trajectories with the same integer part of x. (Again we note that almost all initial conditions lead to the same final physical state of the pendulum, i.e., the same fractional part of x, so that these are not basin boundaries for the physical motion.)

A fractal dimension d of breaks may be defined and calculated by successively examining sub-breaks in the following procedure, which is suggested by the qualitative discussion, above: a long sequence of velocities $\{v_n\}$ is chosen and a uniform grid of m initial points is evolved. The grid is analyzed for breaks in the graph of final versus initial position (as in Fig. 2). One of these break intervals is chosen (at

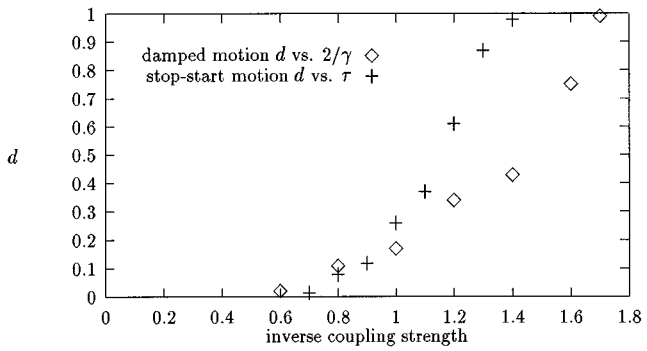

FIG. 4. Fractal dimension d of the break structure, defined in Eq. (9), vs inverse coupling strength, $2/\gamma$ for damped motion and τ for stop-start motion, at temperature $k_BT=1$.

random) and a finer uniform grid of m initial points on that interval is evolved using the *same set* of velocities $\{v_n\}$. This grid of m points is, in turn, analyzed for breaks, one of its break intervals chosen, and m uniformly spaced points on that interval evolved, again using the same velocities $\{v_n\}$, and so on. The fractal dimension is then defined [21] by

$$d=\frac{\ln n_b}{\ln m}, \tag{9}$$

where n_b is the average number of sub-breaks that appear on each grid of m points. For the Langevin implementation of the motion, the fractal dimension of breaks for the constant initial velocity slices, given in Eq. (9), is equal to d_2-1, where d_2 is the fractal dimension of the basin boundaries in the full two-dimensional space of initial conditions $[x,v]$.

The fractal dimension of breaks versus environmental coupling strength is shown in Fig. 4 for a temperature $k_BT=1$. Each point was calculated by averaging d over seven generations of ''sub-breaks'' with $m=100$ (from $\epsilon=10^{-2}$ down to $\epsilon=10^{-14}$) for 100 separate realizations of the random noise. We find that d is zero for values of $1/\gamma$ less than approximately 0.3 and values of τ less than 0.7 and that d approaches 1 near the transition to chaotic behavior for each type of motion. These features will be discussed in detail in Sec. IV C, below.

IV. ANALYTIC RESULTS

A number of features of the behavior of the Lyapunov exponent shown in Fig. 1 and the fractal dimension shown in Fig. 4 can be understood by an analysis of the motion in various limiting cases. First we consider the low-temperature limit, where the system is almost harmonic. Then we examine the regime of strong coupling (i.e., very large γ or very small τ). Finally, we demonstrate some exact results concerning the fractal structure of breaks, calculated numerically in Sec. III B, above, and derive some corresponding results for the Lyapunov exponents at arbitrary temperatures.

A. Low-temperature limit

In the limit $k_BT\ll 1/\pi$, the Boltzmann distribution for the coordinate of the particle is concentrated near $x=0$ and the system is approximately linear, with a force $-\partial V/\partial x\approx -2\pi x$. In this limit, the Lyapunov exponents for the Langevin motion are approximately the same as for damped simple harmonic motion, viz.,

$$\gamma\approx -\frac{\gamma}{2}\pm \mathrm{Re}\sqrt{\frac{\gamma^2}{4}-2\pi}, \tag{10}$$

both of which are negative for all values of γ. Thus, the motion is nonchaotic for arbitrarily weak coupling to the environment at sufficiently low temperatures. We see that taking the larger Lyapunov exponent (+ sign) in Eq. (10) gives a good approximation to λ_1 [see Fig. 1(a)] for the Langevin motion at temperature $k_BT=0.1$. Even at larger temperatures, we see from Fig. 1(a) that the deep minimum in $\lambda_1(\gamma)$ occurs near the critical damping factor $\gamma_c=\sqrt{8\pi}$ for small amplitude motion (or $1/\gamma_c=1/\sqrt{8\pi}=0.1995$).

The low-temperature Lyapunov exponent for stop-start motion may also be calculated exactly [10] and its form reveals the origin of the sharp minima seen in λ of Fig. 1(b). By considering the equations of motion for two trajectories infinitesimally close to $x(t)$, it is straightforward to show that the derivative $f(t)=dx(t)/dx(0)$ satisfies the equation

$$\frac{d^2f}{dt^2}=-K(t)f, \tag{11}$$

where $K(t)=d^2V/dx^2$ at $x=x(t)$, with the initial conditions $f=1$ and $df/dt=0$ at $t=0$. For sufficiently low temperatures, $x\approx 0$ and $K(t)\approx 2\pi$ for all t. Thus, Eq. (11) can be integrated analytically to give $f(t)=\cos(\sqrt{2\pi}t)$ and the low-temperature Lyapunov exponent for stop-start motion, with a time interval τ between collisions, is

$$\lambda(\tau)\approx\frac{1}{\tau}\ln|\cos(\sqrt{2\pi}\tau)|. \tag{12}$$

We see that λ, given in Eq. (12), is always nonpositive and, as in the case of Langevin motion, the system is nonchaotic for arbitrarily weak coupling to the environment at sufficiently low temperature.

The low-temperature approximation of $\lambda(\tau)$ given in Eq. (12) has infinitely deep minima at values of $\tau=P/4,3P/4,5P/4,\ldots$, where $P=\sqrt{2\pi}$ is the period of small-amplitude oscillations about $x=0$. In the harmonic approximation, any two particles started with the same velocity reach precisely the same position at the end of a time interval $\tau=P/4,3P/4,5P/4,\ldots$ This gives rise to the immediate, perfect synchronization achieved by stop-start motion for these values of τ.

At nonzero temperature, these minima are no longer infinite but they remain reasonably close to the values of $\tau=P/4=0.627$, $3P/4=1.88$, etc. As the temperature increases, these minima become less pronounced as the statistical weight of points near $[x,v]=[0,0]$ in the Boltzmann distribution decreases. The low-temperature minima at larger values of τ are more strongly suppressed at high temperatures than the first minimum. This is as one might expect, since nonlinear effects have a larger effect on trajectories integrated over longer times τ.

Although $\lambda(\tau)$ given in Eq. (12) is usually negative, it reaches zero at $\tau=P/2,P,3P/2,\ldots$. This is closely related

to the failure to reach thermal equilibrium, discussed in Ref. [10], for the harmonic oscillator when the time τ is a multiple of the period. Clearly, the change of sign of $\lambda(\tau)$ close to $\tau=1.3$ for nonzero temperatures is strongly associated with the first zero of the low-temperature approximation for $\lambda(\tau)$.

B. Strong-coupling limit

We now consider the system at arbitrary temperature in the very-strong-coupling limit (large γ or small τ). In this limit, the two models give the same largest Lyapunov exponent when $\tau=2/\gamma$. Using the results of Ref. [4], we find that for stop-start motion,

$$\lambda(\tau)\approx-\frac{\tau}{2}\left\langle\frac{\partial^2 V}{\partial x^2}\right\rangle \quad \text{as} \quad \tau\to 0. \tag{13}$$

To calculate the average stretching and contraction of phase-space areas in Langevin motion, we consider the phase-space flow, given by

$$\frac{dx}{dt}=F_x(x,v)=v,$$

$$\frac{dv}{dt}=F_v(x,v)=-\gamma v-\frac{\partial V}{\partial x}.$$

The eigenvalues of $\partial(F_x,F_v)/\partial(x,v)$ are

$$\lambda_{\pm}=-\frac{\gamma}{2}\pm\sqrt{\frac{\gamma^2}{4}-\frac{\partial^2 V}{\partial x^2}}.$$

In the limit $\gamma\gg\sqrt{|\partial^2 V/\partial x^2|}$, one right eigenvector of $\partial(F_x,F_v)/\partial(x,v)$ is approximately aligned with the x axis and the other is approximately along the direction $[1,\gamma]$ in the (x,v) phase space. The eigenvalue associated with the x axis is small, and is approximately

$$\lambda_{+}\approx-\frac{1}{\gamma}\frac{\partial^2 V}{\partial x^2}.$$

The other eigenvalue is large and negative, and is approximately

$$\lambda_{-}\approx-\gamma+\frac{1}{\gamma}\frac{\partial^2 V}{\partial x^2}.$$

Because the right eigenvectors of $\partial(F_x,F_v)/\partial(x,v)$ are approximately independent of time, the Lyapunov exponents of the Langevin motion are equal to the time average of $\lambda_{\pm}$. (The presence of random impulses δv in Langevin motion does not affect the stretching and contraction of phase-space areas since each δv gives a simple shift to all phase-space points: $[x,v]\to[x,v+\delta v]$.) Thus, in the limit $\gamma\gg\sqrt{|\partial^2 V/\partial x^2|}$ for all x, the larger average Lyapunov exponent is given by

$$\lambda_1(\gamma)\approx-\frac{1}{\gamma}\left\langle\frac{\partial^2 V}{\partial x^2}\right\rangle, \tag{14}$$

which is identical to the expression for $\lambda(\tau)$ in Eq. (13), with τ replaced by $2/\gamma$. This is in accord with the derivation of both the Langevin equation and the stop-start motion from the physical model of colliding particles presented in Sec. II.

As the temperature T increases, we see in Fig. 1 that $\lambda(\tau)$ and $\lambda_1(\gamma)$ increase for small values of τ and $1/\gamma$. This is in accord with Eqs. (13) and (14); as the temperature is increased, the average curvature $\partial^2 V/\partial x^2$ decreases because the Boltzmann weight becomes larger near the unstable equilibrium point, $x=1/2$, where the curvature is negative. As $T\to\infty$, all positions x become equally likely and

$$\left\langle\frac{\partial^2 V}{\partial x^2}\right\rangle\to\int_0^1\frac{\partial^2 V}{\partial x^2}\,dx=0.$$

However, as shown in Ref. [4], the thermal average $\langle\partial^2 V/\partial x^2\rangle$ is positive for all finite temperatures, and so the larger Lyapunov exponent is always negative for sufficiently large coupling to the environment.

C. Folding and the structure of breaks

We now turn to consideration of the fractal structure of breaks, for which numerical results were presented in Sec. III. We will demonstrate that the fractal dimension d, defined in Eq. (9), is exactly zero for all values of τ less than $P/4$, where P is the period of small-amplitude oscillations about $x=0$, and for all values of γ greater than the critical damping factor γ_c for small amplitude motion. In doing so, we indirectly demonstrate a much stronger result than that given in Sec. IV B, concerning the sign of the Lyapunov exponents: viz., that the exponents are negative at all temperatures for values of τ less than $P/4$ and for values of γ greater than the critical damping factor $\gamma_c=\sqrt{8\pi}$.

The key analytic result which enables us to derive these results is a type of ''no-folding'' theorem, which states that, given a sequence of velocity impulses ($\{v_n\}$ for stop-start motion or $\{\delta v\}$ for damped motion), the mapping $x(0)\to x(t)$ has positive derivative $dx(t)/dx(0)$ for all $t>0$ when $\tau<P/4$ or $\gamma>\gamma_c$. Thus, the mapping $x(0)\to x(t)$ is always invertible. For damped motion, this result applies to all constant initial velocity slices. This means that the time evolution of a line of initial conditions never ''folds'' the line on top of itself. The importance of folding for the onset of chaos in bounded systems is well known [22]. Since the stop-start motion is one dimensional, invertibility of the map immediately implies that the motion is nonchaotic [23]. In the case of damped motion, we can also show that the motion is nonchaotic for $\gamma<\gamma_c$, but this requires some additional mathematical details, which we defer to the Appendix.

If the mapping $x(0)\to x(t)$ has a positive derivative $dx(t)/dx(0)$ for all $x(0)$ and t (and hence is invertible), then it follows that there is exactly one break (i.e., exactly one unstable trajectory) and the fractal dimension of the set of breaks is zero. To prove this, we note that in the nonchaotic regime, all stable trajectories converge at large times to trajectories $x(t)$ which differ from each other by an integer. Thus, if $x_1(t)$ and $x_2(t)$ are typical trajectories, $x_2(t)-x_1(t)\to n$, an integer, as $t\to\infty$. Now consider the evolution of the line segment [0,1] of initial values of x. If $x_1(0)=0$ and $x_2(0)=1$, then $x_2(t)-x_1(t)=1$ for all $t>0$.

Since $dx(t)/dx(0)$ is always positive, it follows that $x_1(t) < x(t) < x_2(t)$ for all $t > 0$, if $0 < x(0) < 1$. Thus, either $x(t) \to x_1(t)$ or $x(t) \to x_2(t) = x_1(t) + 1$, as $t \to \infty$. In the first case [viz. $x(t) \to x_1(t)$], then $x'(t) \to x_1(t)$, for all $x'(0)$ with $0 < x'(0) < x(0)$. In the second case [viz. $x(t) \to x_1(t) + 1$], then $x'(t) \to x_1(t) + 1$, for all $x'(0)$ with $1 > x'(0) > x(0)$.

From this we see that the line of initial conditions breaks in two at some point x_b: all points greater than x_b converge to $x_2(t)$ and all points less than x_b converge to $x_1(t)$. The point $x(0) = x_b$ is then the initial point of the only unstable trajectory. The location of x_b is determined by the specific sequence of values chosen for the driving impulses of the thermal environment. We note that at zero temperature $x_b = 1/2$, corresponding to the point of unstable equilibrium of the pendulum.

Because of the ergodicity of the Brownian motion, almost all initial conditions lead to trajectories with the same average Lyapunov exponent. Thus, either $|dx(t)/dx(0)| \to \infty$ or $|dx(t)/dx(0)| \to 0$ as $t \to \infty$ for almost all $x(0)$. However, since

$$\int_0^1 \frac{dx(t)}{dx(0)}\, dx(0) = 1 \quad \text{for all } t > 0, \tag{15}$$

only the second option, $|dx(t)/dx(0)| \to 0$ as $t \to \infty$, can occur when $dx(t)/dx(0) > 0$ for all $x(0)$. Thus, it immediately follows that stop-start motion is nonchaotic if the derivative $dx(t)/dx(0)$ is always positive. The corresponding result is proven for Langevin motion in the Appendix.

We now demonstrate that for stop-start motion the mapping $x(0) \to x(t)$ (for any given realization $\{v_n\}$ of the thermal velocities) has positive derivative $f(t) = dx(t)/dx(0)$ if the time τ is less than $P/4$. It suffices to show this result for the first step $t = \tau$ only, since all subsequent steps are equivalent and the derivative $dx(n\tau)/dx(0)$ is the product of the n derivatives $dx(m\tau)/dx((m-1)\tau)$, for $m = 1, \ldots, n$.

It was shown in Sec. IV A that the derivative $f(t)$ satisfies Eq. (11) during the time interval $0 < t < \tau$. The initial conditions are $f = 1$ and $df/dt = 0$ at $t = 0$. Note that the condition, $df/dt = 0$, corresponds to the fact that all trajectories are given the same velocity $dx/dt = v_n$ at the start of each step. Although $K(t)$ depends on the random trajectory followed, it is always less than the maximum curvature of the potential, $K_{\max} = 2\pi$, which occurs when $x(t) = 0$.

To show that the solution of Eq. (11) is always positive for $t < P/4$, we use the standard comparison theorems [24] for linear second-order ordinary differential equations, taking the equation

$$\frac{d^2z}{dt^2} = -K_{\max} z \tag{16}$$

for comparison with Eq. (11). For the purposes of this demonstration, we consider Eq. (11) to be analytically continued [25] to the interval $-\tau \leqslant t < 0$, taking $K(-t) = K(t)$ for $0 \leqslant t \leqslant \tau$. Then, since $df/dt = 0$ at $t = 0$, it follows that $f(-t) = f(t)$ for the analytic continuation of the solution of Eq. (11). If $f(t)$ were zero for any value of $t \in (0, P/4)$, then there would be at least two zeros of the analytically continued f in the interval $-P/4 < t < P/4$. However, the function $\cos(\sqrt{K_{\max}}t)$, which satisfies Eq. (16), has no zeros between $-P/4$ and $+P/4$. This contradicts the comparison theorem [24], which states that, since $K(t) < K_{\max}$ for all t, there is at least one zero of the solution of Eq. (16) between any two zeros of a solution of Eq. (11). Hence, there are no zeros of $f(t)$ in the interval $0 < t < P/4$.

Thus, f is always positive for $\tau < P/4$, and the mapping $x(0) \to x(\tau)$ is invertible. Hence, if $\tau < P/4$, the mapping $x(n\tau - \tau) \to x(n\tau)$ is always invertible (regardless of v_n), the evolution of the system is nonchaotic, and exactly one trajectory is unstable for any set of velocities $\{v_1, v_2, \ldots\}$. The same result is shown in the Appendix for constant initial velocity slices in the Langevin motion with $\gamma > \gamma_c$.

Conversely, for damped motion or stop-start motion, if γ is less than critical damping for harmonic motion or $\tau > P/4$, respectively, the fractal dimension of the break structure is greater than zero. This follows from the fact that the map is not invertible near $x(0) = 0$ for small velocity and folding of the region near $x = 0$ occurs. Because of the ergodicity of the thermal motion, this means folding is possible (at large times) near any point x and multiple breaks will occur in the graph of $x(t \to \infty)$ versus $x(0)$ if a break is created in a region after it has been folded on itself. (Numerically, we find that this is the common mechanism for formation of multiple breaks.) Once multiple breaks are possible, it immediately follows from the statistical homogeneity of the motion in time that the fractal dimension of the break structure is greater than zero.

Near the transition to chaotic behavior, the average Lyapunov exponent over an infinitely long walk is approximately zero. In this regime, two points x_1 and x_2 may remain very close for very long periods of time when the average Lyapunov exponent is negative over that time interval and yet subsequent positive fluctuations in the Lyapunov exponent can lead to a break forming between x_1 and x_2. Thus, in the nonchaotic regime near the transition to the chaotic regime, the fractal dimension of breaks tends to 1 as the probability of a break evolving in any given interval $[x_1(0), x_2(0)]$ at some stage of an infinitely long walk tends to one. On the chaotic side of the transition, the concept of a ''break'' strictly can not be defined in the infinite-time limit since any exponential convergence of two points x_1 and x_2 must be overcome at a later stage by an exponential divergence. However, because the probability distribution of $x_1 - x_2$ is very strongly peaked near 0 when the average Lyapunov exponent is approximately zero (but positive) [3,6], a remanent of break formation can be observed even for large simulation times for small positive Lyapunov exponents.

As a final point relating to the fractal structure of breaks and its relationship to the Lyapunov exponent, we observe that, for stop-start motion, the derivative

$$\frac{d\lambda}{d\tau} \to -\infty \quad \text{at } \tau = P/4.$$

This follows from consideration of the integrand in the expression for $\lambda(\tau)$, given in Eq. (8). The term

$$f(x, v; \tau) = \left.\frac{\partial x(\tau)}{\partial x(0)}\right|_{\substack{x(0)=x \\ v(0)=v}}$$

has a local minimum at $(x=0, v=0)$ for each fixed value of $\tau < P/4$. As τ is increased from zero, $f(0,0;\tau)$ decreases from 1 to 0, crossing $f=0$ for the first time at $\tau = P/4$. Any two-dimensional integral of the form in Eq. (8) will have an infinite negative derivative in τ when the term $f(x,v;\tau)$ in the log first crosses zero. Thus, the transition from fractal dimension $d=0$ to $d>0$ for the structure of breaks is associated with an infinite negative derivative of the Lyapunov exponent λ as a function of the environmental coupling τ. This is seen quite clearly in the numerical results shown in Fig. 1(b).

V. DISCUSSION AND CONCLUSIONS

The striking similarity of the results for stop-start motion and Langevin motion, despite the difference between their formal representation, can be traced to the fact that the ratio of the two Lyapunov exponents for damped motion $\lambda_+(\gamma)/\lambda_-(\gamma) \approx \lambda_+(\gamma)/\gamma$ is usually small, except for $\gamma < \gamma_c$ in the low-temperature, harmonic limit. This means that for Langevin motion the velocity difference of two nearby trajectories decays much more rapidly than the position difference and the phase space is effectively one-dimensional, as it is for stop-start motion. Moreover, on the time-scale defined by $1/\lambda_+(\gamma)$, which determines the convergence of positions in Langevin motion, the time between collisions in stop-start motion with $\tau = 2/\gamma$ is small, so that the difference between continuous (Langevin) damping and sudden (stop-start) damping at intervals of τ is not qualitatively important.

The analysis of the nonchaotic regime of motion for both stop-start and Langevin motion of the simple pendulum reveals that the essential precursor of chaos in this regime is the existence of a set of unstable trajectories. Although these trajectories are exceptional and have no statistical weight in the ''typical'' response of the system to the driving by its thermal environment, they are, nevertheless, highly significant. Although the particular set of points that lead to unstable trajectories depends on the specific realization of the thermal noise, its fractal dimension can be characterized in a statistical sense and the onset of chaos from the nonchaotic regime can be associated with the growth of the fractal dimension from zero to one.

This fractal structure is strongly associated with the folding action of the phase-space dynamics of the system driven by thermal forces. We have seen that when no folding occurs, for each choice of the sequence of environmental driving forces, there is only one initial value of x leading to an unstable trajectory and the system is nonchaotic. The basin boundaries are then simple.

Each basin of attraction corresponds to initial conditions leading to final trajectories with the same integral part of x; in terms of the physical pendulum motion, these basins correspond to trajectories which have the same winding number. As folding and stretching become more effective, and the fractal dimension of the basin boundaries grows, the basins of attraction for different winding numbers become infiltrated into one another. It then takes a longer and longer time for the final winding number of a particular initial condition to be determined. As the transition to chaos is approached, it takes an infinite time for the winding number to be decided.

Although the pendulum has provided a very useful prototype for the analysis of these effects, many of the results obtained above can be extended to arbitrary bounded one-dimensional systems. It is clear that the maximum curvature $K_{\max}$ is the crucial aspect of the potential which ensures that no folding occurs for either stop-start or damped motion. This maximum curvature occurs at the point of stable equilibrium for the pendulum (i.e., the pendulum potential has ''soft'' anharmonicity). This is not true for a general potential. We see from the details of the proofs given for the pendulum that it is the maximum curvature of the potential, rather than the curvature at the stable equilibrium, which in general determines critical values of $\gamma = 2\sqrt{K_{\max}}$ and $\tau = 2\pi/\sqrt{K_{\max}}$. For environmental coupling greater than these critical values of γ or $1/\tau$, the system is nonchaotic at all temperatures.

In conclusion, we have shown that for a pendulum coupled to a thermal environment, the precursor of chaos in the nonchaotic regime is the existence of a fractal set of unstable trajectories for each noise realization. The fractal structure of this set is associated with the folding and stretching action of the phase-space dynamics. The dimension of this set is zero (i.e., exactly one trajectory is unstable) for coupling larger than a critical value in two distinct types of coupling to the environment, damped motion and stop-start motion. The range of values of the environmental coupling for which the fractal dimension is zero (and exactly one trajectory is unstable) does not depend on temperature and bears a strikingly simple relation to elementary characteristic constants of the *small-amplitude* motion about equilibrium: for damped motion, the fractal dimension is zero for all damping rates γ greater than the usual critical damping for small amplitude oscillations; for stop-start motion, the fractal dimension is zero for all stop-start times τ less than $P/4$, where P is the period of small amplitude oscillations. For environmental coupling greater than these values, no folding occurs and the motion is nonchaotic at all temperatures. For environmental coupling less than these critical values, the fractal dimension of the set of initial points of the unstable trajectories grows until it equals 1 at the transition to the chaotic regime. The similarities between damped motion with damping coefficient γ and stop-start motion with $\tau = 2/\gamma$, in terms of the fractal structure and also of the largest Lyapunov exponent, have been investigated numerically and analytically. These results have corresponding generalizations for arbitrary bounded one-dimensional systems.

APPENDIX: ''NO-FOLDING'' THEOREM FOR LANGEVIN MOTION

We first demonstrate that for damped motion the mapping $x(0) \to x(t)$ (for a given noise realization $\{\delta v\}$) has positive derivative $dx(t)/dx(0)$ on each constant initial velocity slice when the damping coefficient $\gamma > \gamma_c$, so that small amplitude motion is overdamped. We then further demonstrate that, in this case, the motion is nonchaotic.

For reference later in the discussion, we consider the time evolution of a more general curve of initial conditions, specified by

$$x(0)=\xi, \quad v(0)=v_0(\xi) \quad \text{for } 0<\xi<1. \tag{A1}$$

The constant initial velocity slices are a particular case of this type of curve of initial conditions, where $v_0(\xi)$ = constant. We define

$$f(\xi;t)=\frac{dx(t)}{d\xi}=\left.\frac{\partial x(t)}{\partial x(0)}\right|_{v(0)}+\frac{dv_0}{d\xi}\left.\frac{\partial x(t)}{\partial v(0)}\right|_{x(0)}. \quad \text{(A2)}$$

By considering the equations of motion for two trajectories with initial conditions along the curve (A1), we find the analog of Eq. (11) for the Langevin motion:

$$\frac{d^2f}{dt^2}=-\gamma\frac{df}{dt}-K(t)f, \quad \text{(A3)}$$

where $K(t)=d^2V/dx^2$ at $x=x(t)$, with the initial conditions $f=1$ and $df/dt=dv_0/d\xi$ at $t=0$. The function $K(t)$ depends on the random trajectory $x(t)$. However, $K(t)$ is never larger than the maximum curvature $K_{\max}=d^2V/dx^2$ of the potential, which occurs at $x=0$.

Defining the function

$$g(\xi;t)=\exp[\gamma t/2]f(\xi;t),$$

we see that g satisfies the equation

$$\frac{d^2g}{dt^2}=\left[\frac{\gamma^2}{4}-K(t)\right]g, \quad \text{(A4)}$$

with initial conditions $g=1$ and $dg/dt=dv_0/d\xi+\gamma/2$ at $t=0$.

For all values of $\gamma>\gamma_c$, the term $[\gamma^2/4-K(t)]$ in Eq. (A4) is always positive. Hence, if $g=1$ and $dg/dt\geq 0$ at $t=0$, $g(t)$ must be positive for all $t>0$. To demonstrate this, suppose on the contrary that $g(t)=0$ for some $t>0$. Assume that the first such zero of g is at $t=t_1$. Then $g(t)>0$ for all $t\in[0,t_1]$. Also, $dg/dt<0$ for $t=t_1$. However,

$$\left.\frac{dg}{dt}\right|_{t=t_1}=\left.\frac{dg}{dt}\right|_{t=0}+\int_0^{t_1}\frac{d^2g}{dt^2}\,dt$$

$$=\left.\frac{dg}{dt}\right|_{t=0}+\int_0^{t_1}\left[\frac{\gamma^2}{4}-K(t)\right]g\,dt. \quad \text{(A5)}$$

This is clearly a contradiction; the left-hand side of Eq. (A5) is negative but the first term on the right-hand side is assumed to be non-negative and the second term is the integral of a positive quantity.

Thus, we obtain the following result for Langevin motion when $\gamma>\gamma_c=2\sqrt{K_{\max}}$: for each value of ξ, the function $f(\xi;t)>0$ for all $t>0$ if the curve of initial conditions satisfies

$$\frac{dv_0}{d\xi}\geq-\gamma/2 \quad \text{(A6)}$$

at that value of ξ.

We now apply this result to the constant velocity slices, for which $dv_0/d\xi=0$. These slices of initial conditions clearly satisfy Eq. (A6) for all ξ. We now have that $dx(\tau)/dx(0)=dx(\tau)/d\xi>0$, which was the ''no-folding'' condition we wished to demonstrate. Moreover, along any constant velocity slice, Eq. (15) is valid. This then leads to the conclusion that, for almost all initial conditions

$$\left.\frac{\partial x(t)}{\partial x(0)}\right|_{v(0)}\to 0 \quad \text{as} \quad t\to\infty, \quad \text{(A7)}$$

i.e., the final position is not sensitive to the initial position when $\gamma>\gamma_c$.

By considering a curve of initial conditions with $dv_0/d\xi=-\gamma/2$, we see that

$$\left.\frac{\partial x(t)}{\partial x(0)}\right|_{v(0)}-\frac{\gamma}{2}\left.\frac{\partial x(t)}{\partial v(0)}\right|_{x(0)}>0, \quad \text{(A8)}$$

for all initial conditions. Similarly, considering a curve of initial conditions with $dv_0/d\xi=\gamma/2$, we see that

$$\left.\frac{\partial x(t)}{\partial x(0)}\right|_{v(0)}+\frac{\gamma}{2}\left.\frac{\partial x(t)}{\partial v(0)}\right|_{x(0)}>0. \quad \text{(A9)}$$

Combining Eqs. (A8) and (A9), we find the general result for Langevin motion:

$$\left|\left.\frac{\partial x(t)}{\partial x(0)}\right|_{v(0)}\right|>\frac{\gamma}{2}\left|\left.\frac{\partial x(t)}{\partial v(0)}\right|_{x(0)}\right|, \quad \text{(A10)}$$

for all initial conditions when $\gamma>\gamma_c$. From Eqs. (A7) and (A10), it follows that

$$\left.\frac{\partial x(t)}{\partial v(0)}\right|_{x(0)}\to 0 \quad \text{as} \quad t\to\infty, \quad \text{(A11)}$$

for almost all initial conditions when $\gamma>\gamma_c$.

Equations (A7) and (A11) express the fact that the final position $x(t)$ is insensitive to the initial position $x(0)$ and velocity $v(0)$, respectively. Differentiating these two equations with respect to t demonstrates that the final velocity $v(t)$ is also insensitive to the initial position and velocity. This completes the proof that the final phase-space coordinates, given a particular realization of thermal impulses $\{\delta v\}$ in Langevin motion, are insensitive to the initial conditions for almost all trajectories when the damping factor $\gamma>\gamma_c$. Thus, the Langevin motion is nonchaotic at arbitrary temperatures for all $\gamma>\gamma_c$.

[1] B. Derrida and G. Weisbuch, Europhys. Lett. **4**, 657 (1987).
[2] H. Herzel and B. Pompe, Phys. Lett. A **122**, 121 (1987).
[3] L. Yu, E. Ott, and Q. Chen, Phys. Rev. Lett. **65**, 2935 (1990).
[4] S. Fahy and D. R. Hamann, Phys. Rev. Lett. **69**, 761 (1992).
[5] G. Björk, Phys. Rev. A **45**, 8259 (1992).
[6] A. S. Pikovsky, Phys. Lett. A **165**, 33 (1992).
[7] S. Sinha, Phys. Rev. Lett. **69**, 3306 (1992).
[8] A. Maritan and J. R. Banavar, Phys. Rev. Lett. **73**, 1451 (1994).
[9] A. S. Pikovsky, Phys. Rev. Lett. **73**, 2931 (1994); A. Maritan

and J. R. Banavar, *ibid.* **73**, 2932 (1994).
[10] E. Barkai and V. Fleurov, Phys. Rev. E **52**, 137 (1995).
[11] Y.-Y. Chen, Phys. Rev. Lett. **77**, 1451 (1996).
[12] E. G. Gwinn and R. M. Westervelt, Phys. Rev. Lett. **54**, 1613 (1985); Phys. Rev. A **33**, 4143 (1986).
[13] S. Chandrasekar, Rev. Mod. Phys. **15**, 1 (1943).
[14] H. Risken, *The Fokker-Planck Equation*, 2nd ed. (Springer, Berlin, 1989), Chap. 3.
[15] S. Duane, A. D. Kennedy, B. J. Pendleton, and D. Roweth, Phys. Lett. B **195**, 216 (1987), and references therein.
[16] D. R. Hamann and S. Fahy, Phys. Rev. B **47**, 1717 (1993).
[17] W. H. Press *et al.*, *Numerical Recipes–The Art of Scientific Computing* (FORTRAN *version*) (Cambridge University Press, 1989), p. 199.
[18] D. E. Knuth, *Seminumerical Algorithms*, 2nd ed. (Addison-Wesley, Reading, MA, 1981).
[19] It follows directly from Eq. (4) that the sum of the two Lyapunov exponents for Langevin motion along any trajectory is always $-\gamma$, so that once the larger exponent is known, the other can be found immediately.
[20] This transient divergence behavior is a precursor of the intermittent bursting in the chaotic regime discussed in Ref. [3].
[21] C. Grebogi, E. Ott, and J. A. Yorke, Science **238**, 632 (1987).
[22] S. Smale, in *Differential and Combinatorial Topology*, edited by S. S. Cairns (Princeton University Press, Princeton, 1963).
[23] G. L. Baker and J. P. Gollub, *Chaotic Dynamics: An Introduction* (Cambridge University Press, 1990), p. 90.
[24] E. A. Coddington and N. Levinson, *Theory of Ordinary Differential Equations* (McGraw-Hill, New York, 1955), Chap. 8.
[25] Note that this is a purely formal device, since we are interested in the values of $f(t)$ only in the interval $0 \leqslant t \leqslant \tau$. We are not assuming that the actual motion satisfies $K(-t)=K(t)$.